

## Origin of the Hard X-ray Emission from the Galactic Plane

Ken Ebisawa<sup>1\*</sup>, Yoshitomo Maeda<sup>2</sup>, Hidehiro Kaneda<sup>3</sup>, Shigeo Yamauchi<sup>4</sup>

The Galactic plane is a strong hard x-ray emitter and the emission forms a narrow continuous ridge (1-3). The currently known hard x-ray sources are far too few to explain the ridge x-ray emission, and the fundamental question as to whether the ridge emission is ultimately resolved into numerous dimmer discrete sources or truly diffuse emission has not yet been settled (4-9). In order to obtain a decisive answer, using the Chandra x-ray observatory, we have carried out the deepest hard x-ray survey of a Galactic plane region which is devoid of known x-ray point sources. We have detected at least 36 new hard x-ray point sources in addition to strong diffuse emission within a  $17' \times 17'$  field of view. The surface density of the point sources is comparable to that at high Galactic latitudes after the effects of Galactic absorption are considered. Therefore, most of these point sources are probably extragalactic, presumably active galaxies seen through the Galactic disk. The Galactic ridge hard x-ray emission is diffuse, which indicates omnipresence of the hot plasma along the Galactic plane whose energy density is more than

---

<sup>1</sup> code 662, NASA/GSFC, Greenbelt, Maryland 20771, USA, and Universities Space Research Association

<sup>2</sup> Department of Astronomy & Astrophysics, Pennsylvania State University, 525 Davey Lab., University Park, Pennsylvania 16802, USA: Present address; Institute of Space and Astronautical Science, 3-1-1 Yoshinodai, Sagamihara, Kanagawa 229-8510, Japan

<sup>3</sup>Institute of Space and Astronautical Science, 3-1-1 Yoshinodai, Sagamihara, Kanagawa 229-8510, Japan

<sup>4</sup>Faculty of Humanities and Social Sciences, Iwate University, 3-18-34 Ueda, Morioka, Iwate 020-8550, Japan

\* To whom correspondence should be addressed. E-mail: ebisawa@gsfc.nasa.gov

**one order of magnitude higher than any other substances in the interstellar space.**

The Galactic ridge x-ray emission exhibits emission lines from highly ionized heavy elements such as Si, S and Fe, hence it may be considered from optically thin hot plasmas with a temperature of several keV (3). If the plasma distribution is diffuse in the Galactic disk, the plasma temperature is higher than that can be bound by Galactic gravity, and its energy density,  $\sim 10 \text{ eV/cm}^3$ , is one or two orders of magnitude higher than those of other constituents in the interstellar space, such as cosmic rays, Galactic magnetic fields, and ordinary interstellar medium (3, 8). Another hypothesis is that the Galactic ridge x-ray emission is a superposition of numerous point sources (1, 4, 5, 6). However, no class of x-ray objects is known with such a high plasma temperature and a large number density to satisfy the uniform surface brightness of the ridge emission (8, 9).

To resolve the origin of the Galactic ridge x-ray emission, we observed a “blank” region of the Galactic plane,  $(l, b) \approx (+28^\circ.45, -0^\circ.2)$ , where the Advanced Satellite for Cosmology and Astrophysics (ASCA) could not find any point sources (7, 8) brighter than  $\sim 2 \times 10^{-13} \text{ erg s}^{-1} \text{ cm}^{-2}$  (2 – 10 keV). We used the Advanced CCD Imaging Spectrometer Imaging-array (ACIS-I) onboard the Chandra Observatory, with unprecedented sensitivity and imaging quality (Fig. 1). The observation was carried out on 25 and 26 February, 2000, for a total exposure time of 90 ksec. The pointing position was chosen because the direction is tangential to the Scutum arm where the ridge x-ray emission is strong.

We were interested in hard x-ray emission, so we searched in the 3 – 8 keV band to minimize the effects of Galactic absorption at lower energies and the intrinsic non-x-ray background in the higher energy band. The “wavdetect”

source finding program in the Chandra data analysis package detected 53, 36 and 29 sources in the  $17' \times 17'$  ACIS-I field with 3, 4 and 4.5  $\sigma$  significance, respectively. For each of these sources, we determined the energy flux in the 2 – 10 keV band by fitting the energy spectrum after accounting for the position dependent detector responses. The 3, 4 and 4.5  $\sigma$  thresholds roughly correspond to energy fluxes of  $\sim 3 \times 10^{-15}$ ,  $\sim 4 \times 10^{-15}$  and  $\sim 5 \times 10^{-15}$  ergs s $^{-1}$  cm $^{-2}$  in the 2 – 10 keV band, respectively. We found point sources with different fluxes are randomly distributed over the field of view, which indicates that the positional dependence of the source detection efficiency is negligible. We have also carried out a source search in the 0.5 – 3 keV soft x-ray band, and detected 106 sources with 3  $\sigma$  confidence. There are only 17 sources which are detected both in the hard and soft band over 3  $\sigma$  confidence, which suggests that the populations of the soft sources and hard sources are different. We identified several soft x-ray sources, which are not detected in the hard band, with objects in the United States Naval Observatory A2.0 catalog and/or the Palomar Digital Deep Sky Survey; thus these sources are probably ordinary stars. On the other hand, none of the hard x-ray sources we observed have been identified.

Chandra data consist of not only x-ray events from point sources and diffuse emission, but also non-x-ray background events. Typical non-x-ray background rate has been calculated and released by Chandra X-ray Center, based on observations of source-free high Galactic latitude regions. By subtracting the expected non-x-ray background rate, we have determined the total hard x-ray flux in our field of view as  $\sim 1.1 \times 10^{-10}$  ergs s $^{-1}$  cm $^{-2}$  deg $^{-2}$  in 2 – 10 keV, which includes contributions from both diffuse emission and point sources. On the other hand, integrated hard x-ray flux of all the point sources above the flux  $3 \times 10^{-15}$  ergs s $^{-1}$  cm $^{-2}$  is  $\sim 9.8 \times 10^{-12}$  ergs s $^{-1}$  cm $^{-2}$  deg $^{-2}$  (2 – 10 keV), which is only  $\sim 10$  % of the total observed x-ray flux in the field of view, and

the rest is the diffuse emission (Fig. 1 and 2).

The point x-ray sources on the Galactic plane may comprise extragalactic sources seen through the Galactic plane and Galactic sources. Remarkably, the surface density of the hard x-ray sources on the Galactic plane we have determined is consistent with that of the high Galactic latitude fields in a similar flux range (Fig. 2). The x-ray fluxes of extragalactic sources are reduced on the Galactic plane because they are absorbed by interstellar matter. The Galactic HI column density in our Chandra pointing direction is  $\sim 2 \times 10^{22} \text{ cm}^{-2}$  (12) and that of the molecular hydrogen is  $(1 - 2) \times 10^{22} \text{ cm}^{-2}$  (13), both measured from radio observations (12, 13). Therefore, the total hydrogen column density through the Galactic plane is  $N_H = N_{HI} + 2N_{H_2} = (4 - 6) \times 10^{22} \text{ cm}^{-2}$ . Even if we account for the  $\sim 30\%$  flux reduction of the extragalactic hard x-ray sources caused by the interstellar absorption of  $N_H = 6 \times 10^{22} \text{ cm}^{-2}$ , the extragalactic  $\log N - \log S$  curve is still consistent with the present Chandra Galactic  $\log N - \log S$  curve within 90 % statistical uncertainty (Fig. 2). Therefore, most of the point sources detected in our field must be extragalactic, presumably Active Galactic Nuclei, which dominate the cosmic x-ray background (10).

From our observation, the point source density on the Galactic plane in the flux range above  $3 \times 10^{-15} \text{ ergs s}^{-1} \text{ cm}^{-2}$  (2 - 10 keV) is  $660 \pm 160 \text{ sources/deg}^2$  (90 % error), among which  $\sim 560 \text{ sources/deg}^2$  is considered to be the extragalactic sources (10), where we took account of the  $\sim 30\%$  flux reduction due to the Galactic absorption. This suggests that there would be at most  $\sim 260 \text{ sources/deg}^2$  Galactic sources at this flux level, which corresponds to a  $\sim 4 \times 10^{31} \text{ erg s}^{-1}$  source at 10 kpc assuming isotropic emission. X-ray luminosity functions and spatial densities of quiescent dwarf novae have not been measured precisely (4, 6), and our results can place an upper-limit for the quiescent dwarf nova population. For example, a combination of a  $10^{-5} \text{ pc}^{-3}$  spatial density

and  $10^{31}$  erg s $^{-1}$  average luminosity of quiescent dwarf novae, which amounts to  $\sim 1000$  sources/deg $^2$  at  $> 3 \times 10^{-15}$  ergs s $^{-1}$  cm $^{-2}$  (7), is clearly ruled out. To be consistent with our observation, either spatial density or average luminosity has to be smaller at least by a factor of four.

The paucity of Galactic point sources supports models of diffuse emission to explain the Galactic ridge x-ray emission. Then the next question is how to produce plasmas with such a large energy density and high temperatures, and keep them in the Galactic disk. Theories have been proposed to explain these problems in terms of interstellar-magnetic reconnection (14), interaction of energetic cosmic-ray electrons (15) or heavy-ions (16) with interstellar medium. All of these models require supernovae as a mechanism of the energy input. Incidentally, in the region around  $(l, b) \approx (28^\circ.55, -0^\circ.12)$ , we found an extended feature with a size of  $\sim 2'$  which is more conspicuous in the hard x-ray band than in the soft band (Fig. 3). This region corresponds to the southern end of an extended and patchy radio source named G28.60–0.13 (17), and the diffuse x-ray structure we found bridges three discrete radio patches F, G and H (17). A high quality x-ray spectrum of the G28.60–0.13 region by the ASCA satellite indicates that the energy spectrum is a single power-law without any iron line emissions (18), which is reminiscence of the non-thermal acceleration taking place in the supernova remnants such as SN1006 (19) or RX J1713.7-3946 (20). The extended feature at  $(l, b) \approx (28^\circ.55, -0^\circ.12)$ , or G28.60–0.13 itself, may be an aged supernova remnant. Supernova remnants may be ubiquitous on the Galactic plane (17) and these remnants may have an important role to generate the Galactic ridge hard x-ray emission (21).

## References and Notes

1. D. M. Worrall, F. E. Marshall, E. A. Boldt, J. H. Swank, *Astrophys. J.* **255**, 111 (1982).
2. R. S. Warwick, M. J. L. Turner, M. G. Watson, R. Wilingale, *Nature* **317**, 218 (1985).
3. K. Koyama *et al.*, *Publ. Astro. Soc. Japan* **38**, 121 (1986).
4. K. Mukai, K. Shiokawa, *Astrophys. J.* **418**, 863 (1993).
5. R. Ottmann, J. H. M. M. Schmitt, *Astron. & Astrophys.* **256**, 421 (1992).
6. M. G. Watson, in “Annapolis Workshop on Magnetic Cataclysmic Variable”, ASP Conference Series, vol. 157, 1999, p.291.
7. S. Yamauchi *et al.*, *Publ. Astro. Soc. Japan* **48**, L15 (1996).
8. H. Kaneda *et al.*, *Astrophys. J.* **491**, 638, (1997).
9. M. Sugizaki *et al.*, *Astrophys. J. Supp.* **134**, 77 (2001)
10. R. Giacconi *et al.*, *Astrophys. J.* **551**, 624 (2001)
11. Y. Ueda, *et al.*, *Astrophys. J.* **518**, 656 (1999)
12. J. M. Dickey, F. J. Lockman, *Ann. Rev. Astro. Astrophys.* **28**, 215 (1990).
13. T. M. Dame, D. Hartmann, P. Thaddeus, *Astrophys. J.* **547**, 792 (2001)
14. S. Tanuma, *et al.*, *Publ. Astro. Soc. Japan* **51**, 161 (1999)
15. A. Valinia *et al.*, *Astrophys. J.* **543**, 733 (2000)
16. Y. Tanaka, T. Miyaji, G. Hasinger, *Astronomische Nachrichten* **320**, 181 (1999)
17. D. J. Helfand, T. Velusamy, R. H. Becker, F. J. Lockman, *Astrophys. J.* **341**, 151 (1989)
18. A. Bamba, *et al.*, *Publ. Astro. Soc. Japan* **53**, accepted (2001)
19. K. Koyama, *et al.*, *Nature* **378**, 255 (1995)
20. K. Koyama, *et al.*, *Publ. Astro. Soc. Japan* **49**, L7 (1997)
21. K. Koyama, S. Ikeuchi and K. Tomisaka, *Publ. Astro. Soc. Japan* **38**, 503

(1986)

22. We are grateful to Drs. F. E. Marshall, K. Mukai, and R. F. Mushotzky for helpful comments which improved an earlier version of this Report. We also thank Prof. Y. Tanaka and other anonymous referees for useful comments. The observation was carried out under NASA's Chandra Guest Observer Program.

Figure 1: The *Chandra* ACIS-I deep exposure image on the Galactic plane. Original image has been smoothed with an adaptive filter to make both the point sources and diffuse emission clearly visible. Color and contrast are adjusted so that the point sources detected in the 0.5–3 keV band and the 3 – 8 keV band are conspicuous in red and blue, respectively. The hard x-ray diffuse emission is shown in blue. The image has  $690 \times 690$  pixels with the pixel size  $1.''97$  square.



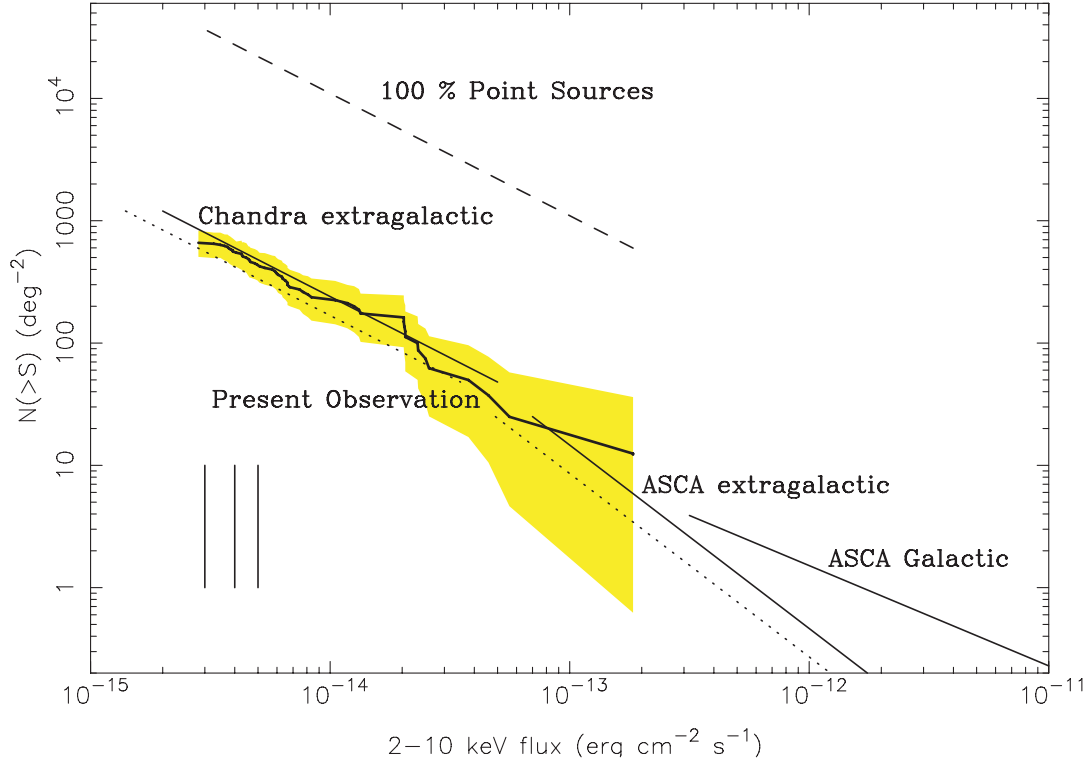


Figure 2: The number of point sources per unit area,  $N$ , brighter than the threshold flux in the 2 – 10 keV band,  $S$ , is indicated as a function of  $S$  (the  $\log N - \log S$  curve). The present Chandra  $\log N - \log S$  curve on the Galactic plane is shown with the thick line, and the 90 % error region (assuming Poisson counting error) is indicated in yellow. The upper dashed line shows the number of fictitious point sources at a given flux  $S$  that would have accounted for the total observed x-ray energy flux in the Chandra field of view ( $\sim 1.1 \times 10^{-10}$  ergs  $\text{s}^{-1} \text{cm}^{-2} \text{deg}^{-2}$  in 2 – 10 keV). Three vertical lines at lower-left indicate the threshold energy fluxes corresponding to 3, 4 and 4.5  $\sigma$  confidence of the source detection. For comparison, the Galactic  $\log N - \log S$  curve by ASCA (9) and extragalactic ones by Chandra (10) and ASCA (11) are shown. The extragalactic  $\log N - \log S$  curves corrected for the effect of  $\sim 30$  % flux reduction due to Galactic absorption with  $N_H = 6 \times 10^{22} \text{cm}^{-2}$  are indicated with dotted line, which are consistent with the present Galactic  $\log N - \log S$  curve within 90 % statistical error.

Figure 3: Close-up of the diffuse feature at around  $(l, b) \approx (28^\circ.55, -0^\circ.12)$ . The 0.5 – 3 keV image is represented in red and the 3 – 8 keV image is in blue, and both images are smoothed so as to enhance the diffuse feature. Contour map of the 3 – 8 keV image is superimposed. Point sources detected with more than 3  $\sigma$  confidence either in the 0.5 – 3 keV band or the 3 – 8 keV band are indicated with crosses. The image has  $560 \times 560$  pixels with the pixel size  $0.''98$  square.

This figure "fig1.jpg" is available in "jpg" format from:

<http://arxiv.org/ps/astro-ph/0108406v1>

This figure "fig3.jpg" is available in "jpg" format from:

<http://arxiv.org/ps/astro-ph/0108406v1>